High-Field Magnetic Birefringence Study of the Structure of Rodlike Phages Pf1 and fd in Solution

J. TORBET and G. MARET, *Hochfeld-Magnetlabor des Max-Planck-Institutes für Festkörperforschung, 166X, F-38042 Grenoble, Cédex, France*

Synopsis

The magnetic orientation of the rodlike bacterial viruses Pf1 and fd in dilute aqueous solution was detected by high-resolution birefringence measurements. Partial alignment takes place parallel to the magnetic field chiefly due to the diagmagnetic anisotropy of the highly ordered α-helices in the coat protein. It follows from the analysis of the experimental diamagnetic anisotropy that in both phages the α-helices and aromatic amino acids are oriented relatively parallel to the phage axis. In Pf1 these become, on average, more nearly parallel as the temperature is reduced from about 25 to 5°C. These results demonstrate that high-resolution magnetically induced birefringence measurements can be used to investigate some general structural features of complicated biological particles in solution.

INTRODUCTION

Pf1 and fd are strains of rodlike single-stranded DNA containing bacteriophages. They both have a diameter of 60 Å, but the length of Pf1 (19,600 Å) is more than twice that of fd (8800 Å). The molecular weight of Pf1 is 37.5×10^6 (fd, 16.4×10^6); it is composed of 7600 (fd, 2700) major coat protein molecules and 7400 (fd, 6400) nucleotides.[1–5] The Pf1 major coat protein consists of 46 (fd, 50) amino acids, of which 2 (fd, 6) are aromatic.[6–8] In addition to the major coat protein, each virus contains 2 to 4 copies of the 50,000 molecular weight A protein,[9] and other minor proteins are probably present.[10]

From x-ray fiber diffraction patterns of Pf1, low-resolution models have been proposed in which the DNA is encapsulated in a helical shell of coat proteins.[11–16] Recent improvements have been made in the analysis of the diffraction pattern.[15,16] In this model the major coat proteins are composed of two nearly equal α-helical sections linked by a small nonhelical region.[16] The α-helices are tilted at an average angle of slightly less than 20° to the virus long axis. It has been suggested from the x-ray work on fibers that Pf1 and fd have similar structures.[11] However, physical and chemical measurements made on solutions indicate that there may be significant structural differences between both phages in solution.[1–5]

Both of these phages can be fully oriented magnetically in solutions above a concentration of about 9 mg/ml (partly reported in Ref. 17). This observation led to the production of fibers with improved orientation,[18] which have been used to further structural studies.[19]

Biopolymers, Vol. 20, 2657–2669 (1981)

CCC 0006-3525/81/122657-13$01.30

We have used magnetically induced birefringence measurements (the classical "Cotton-Mouton" effect) to investigate the average orientation of different molecular groups in Pf1 and fd in dilute solution. The diamagnetic and optical anisotropies per virus are reported and interpreted by geometrically summing the diamagnetic and optical anisotropies of the major coat protein α-helices and aromatic amino acid residues, and of the DNA bases. An approximate estimate of the average orientations of the above groups is made. The diamagnetic anisotropy of a single virus is shown to be largely due to the α-helical peptide bonds. When solutions of Pf1 are cooled, a structural transition is observed to occur between 25 and 5°C. The results demonstrate that magnetically induced birefringence can be used to gain information about some general structural features and that this technique is very sensitive to structural changes. Finally, the anisotropy of the optical polarizability of an α-helical peptide bond is approximately estimated.

PRINCIPLES

This paper is concerned with dilute solutions of rodlike particles which have a diamagnetic susceptibility and optical polarizability that are rotationally symmetric about the particle long (or major) axis. Let $\Delta\chi$ and $\Delta\alpha$ be respectively the difference between the axial and radial values of the diamagnetic susceptibility and optical polarizability of a single rod.

In a solution of fully aligned rods the optical birefringence for light propagating perpendicular to the rod long axis attains a maximum or saturation value Δn_{sat}. If $n_\parallel$ and $n_\perp$ are respectively the refractive indices for light of wavelength, λ, linearly polarized parallel and perpendicular to the rod long axis, then $\Delta n_{sat} = (n_\parallel - n_\perp)_{sat}$. In a dilute solution of mean refractive index n_0 containing R rods per unit volume, the Lorentz-Lorenz formula gives

$$\Delta n_{sat} = \frac{2\pi}{9} \frac{(n_0^2 + 2)^2}{n_0} R\Delta\alpha \tag{1}$$

$R = cN_A/M_r$ where c is the concentration, N_A is Avogadro's number, and M_r is the molecular weight. At low concentration the refractive index of the solution is near to that of water, $n_0 = 1.33$. Hence for a fully aligned sample of known concentration, $\Delta\alpha$ is obtained from a measurement of Δn_{sat}.

When alignment is incomplete the birefringence is reduced and $\Delta n = \phi\Delta n_{sat}$ where ϕ ($0 \leqslant \phi \leqslant 1$) is defined as the degree of orientation. In a magnetic field H that causes only a small degree of alignment, it follows from Langevins orientational theory (e.g. Refs. 20, 21) that $\phi = \Delta\chi H^2/15kT$, where T is the absolute temperature and k is the Boltzmann constant. Hence,

$$\Delta n = \frac{2\pi}{135} \frac{(n_0^2 + 2)^2}{n_0} \frac{H^2}{kT} \frac{cN_A}{M_r} \Delta\chi\Delta\alpha \tag{2}$$

The magnetic field causes the particles to rotate slightly so that, on average, the axis of smallest numerical diamagnetic susceptibility becomes nearer to the field direction.

A classical method for investigating magnetic anisotropies is to measure the birefringence of solutions in a magnetic field. It is called the Cotton-Mouton effect. The induced birefringence Δn in a magnetic field at right angles to the direction of the light ray is given by

$$\Delta n = CM\lambda H^2 \tag{3}$$

where CM is the Cotton-Mouton constant.[20,21] Combining Eqs. (2) and (3),

$$CM = \frac{2\pi}{135}\frac{(n_0^2+2)^2}{n_0}\frac{1}{\lambda kT}\frac{cN_A}{M_r}\Delta\chi\Delta\alpha \tag{4}$$

and Eqs. (1) and (4),

$$\Delta\chi = CM15\lambda kT/\Delta n_{\text{sat}} \tag{5}$$

Thus, $\Delta\chi$ can be obtained from Eq. (5) without knowledge of the absolute concentration.

Both anisotropies, $\Delta\chi$ and $\Delta\alpha$, can have both a shape and intrinsic component. The shape anisotropies, $\Delta\chi_s$ and $\Delta\alpha_s$, result from the particles being nonspherical and having a mean magnetic susceptibility and optical polarizability different from those of the solvent. Usually $\Delta\chi_s$ is very small, and for a phage we estimate, using the equation of Neurath,[22] that it is smaller than the intrinsic value of a single aromatic ring and can therefore be neglected. However, $\Delta\alpha_s$ may be significant and is estimated later in the Results section. The intrinsic diamagnetic anisotropy is due to the composition and relative orientation of the constituents, and to a good approximation it can be written as the geometric sum of the intrinsic anisotropies of the individual components (Pascal's additivity law).[23–25] The major contributions to the intrinsic anisotropies come from the α-helices (subscript α) and the aromatic amino acid residues (subscript a) of the major coat protein and from the DNA bases (subscript D). This is justifiable because other bond anisotropies are known to be considerably smaller.[25] The contributions of the minor capsid proteins are neglected because they constitute only about 1% of a virus. Hence,

$$\Delta\chi = f_\alpha N_\alpha \Delta\chi_\alpha + f_a N_a \Delta\chi_a + f_D N_D \Delta\chi_D \tag{6}$$

and similarly to a first approximation:

$$\Delta\alpha = f_\alpha N_\alpha \Delta\alpha_\alpha + f_a N_a \Delta\alpha_a + f_D N_D \Delta\alpha_D + \Delta\alpha_s \tag{7}$$

The intrinsic anisotropies $\Delta\chi_i$, $\Delta\alpha_i$ ($i = \alpha, a, D$) are referred to the symmetry axis of the molecular group, which is along the length of an α-helix and perpendicular to the plane of an aromatic group. N_i designates the total number of each sort of molecular group per virus and f_i ($1 \geq f_i \geq -0.5$) is given by $f_i = 1.5\cos^2\theta_i - 0.5$, where θ_i ($90° \geq \theta_i \geq 0°$; $f_i = 0$ when $\theta_i \sim 55°$)

is the angle between the molecular group symmetry axis and the virus long axis (see insert in Fig. 3). Equation (7) is approximate, since the optical and shape anisotropies are not exactly additive.[26] Nevertheless, it is adequate for the approximate estimate of $\Delta\alpha_\alpha$ presented here.

If the rods are flexible, the measured Cotton-Mouton constant will be less than the stiff rod value, and a factor related to the degree of flexibility must be introduced into the analysis. Fortunately fd appears to be quite rigid in solution,[2] and a small degree of flexibility would not markedly alter the conclusions. There is no similar data on Pf1, so we have first carried out the analysis assuming it to be a rigid rod and afterwards discuss qualitatively the influence of flexibility on the results.

MATERIALS AND METHODS

The phages prepared as described in Ref. 11 were a gift from Dr. D. A. Marvin. The concentration of the virus solutions (0.01*M* Tris-HCl, pH 7.5) was determined spectrophotometrically using an extinction coefficient at 270 nm of 2.05 cm^2/mg for Pf1 and 3.84 cm^2/mg for fd. The concentration varied from 0.02 to 2 mg/ml. The Cotton-Mouton measurements were made with quartz cells with a 3-cm path length. These were placed in a temperature-stabilized (±0.1°C) sample holder in a Bitter-type magnet [maximum field 13.5 teslas (T); 1 T = 10^4 G] which had a small radial optical bore. The magnetic birefringence Δn was measured with good sensitivity (resolution $\Delta n \sim 10^{-10}$, λ = 6328 Å) using a combined photoelastic modulation and compensation technique.[27] Polarizer and analyzer are crossed and at 45° with respect to the field direction. A small 50-kHz modulation of the birefringence is produced by a photoelastic modulator resulting in a 100-kHz intensity modulation of the photodiode output. Any superimposed steady-state (magnetic) birefringence produces an additional 50-kHz photodiode output which is phase-sensitively detected, dc-converted, and used (as error signal in a feedback loop) to compensate the steady-state birefringence by means of a POCKELS-cell. Hence, in the compensated case the voltage across the POCKELS-cell is a direct measure of the magnetic birefringence Δn. In order to measure the large birefringences given by fully aligned samples (Δn_{sat}), the POCKELS-cell was replaced by an electrically driven Babinet-Soleil compensator and a superconducting magnet with a maximum field of 7 T was used.

RESULTS AND DISCUSSION

Solution Structure of Pf1 and fd

Figure 1 shows typical magnetic birefringence data on dilute solutions of Pf1 and fd. No saturation of Δn was observed even in the highest magnetic fields, indicating that only partial orientation of the viruses took place. The magnetic birefringence of both phage is positive. We find, in

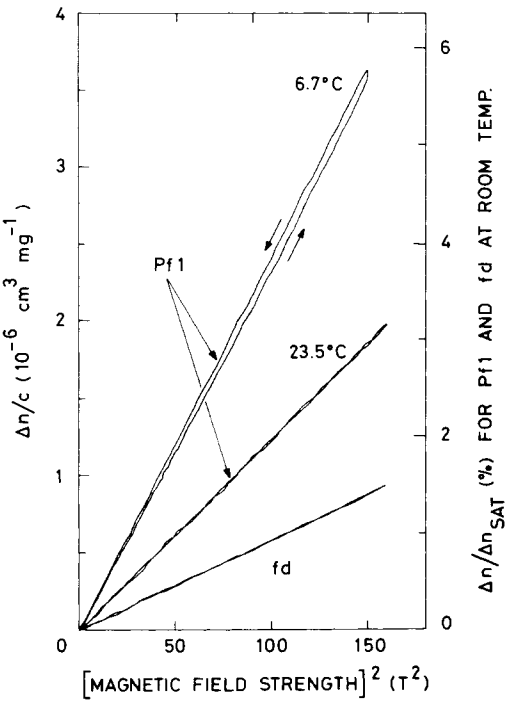

Fig. 1. Continuously measured magnetic birefringence Δn of dilute aqueous solutions of cylindrical bacteriophages Pf1 (concentration, c = 0.31 mg/ml) and fd (c = 1.22 mg/ml) at 22°C on the left-hand scale. The degree of alignment ϕ, as defined in the text, is given on the right-hand scale for fd and Pf1 at room temperature. It took 120 s to sweep the field up and down.

agreement with reported birefringence measurements on fd fibers,[28] that shear-aligned solutions are positively birefringent with respect to the direction of shear. Therefore, both Pf1 and fd orient parallel to the magnetic field. The axis of smallest numerical diamagnetic susceptibility is therefore parallel to the virus long axis and $\Delta\chi$ is positive.

The specific Cotton-Mouton constant, CM/c (Fig. 2), is independent of concentration c, which demonstrates that interparticle interactions are weak under these conditions. However, above a critical concentration (about 7 mg/ml for Pf1 and 10 mg/ml for fd), there is an abrupt transition to a solution of birefringence domains composed of nearly parallel rods. This is due to strong interaction, probably mainly electrostatic repulsion, between the phages. Cooperative behavior results, and so full alignment can be attained and Δn_{sat} measured (Fig. 3). Thus, $\Delta\chi$ can be determined (1.22×10^{-23} J T^{-2} for Pf1; 0.63×10^{-23} J T^{-2} for fd) from Eq. (5).

The $\Delta\chi$ values are now interpreted using Eq. (6) in terms of the average orientation of the molecular groups. The number of each molecular group, N_i, is reliably known from the information quoted in the Introduction. In Pf1 there are 3.5×10^5 α-helical peptides N_α, 15,200 aromatic amino acids N_a, and 7400 DNA bases N_D; and in fd, $N_\alpha = 1.35 \times 10^5$, N_a = 16,200, and

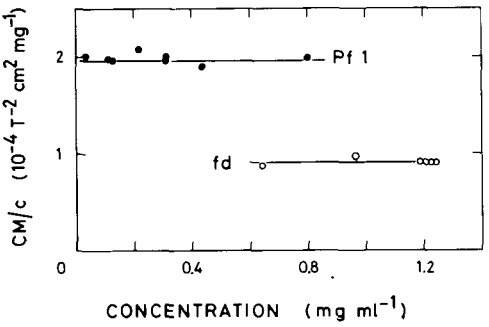

Fig. 2. Concentration dependence of the specific Cotton-Mouton constant (CM/c) for aqueous solutions of Pf1 and fd at room temperature. For Pf1, $CM/c = (1.97 \pm 0.1) \times 10^{-4}$ T^{-2} cm^2 mg^{-1}; and for fd, $CM/c = (0.97 \pm 0.05) \times 10^{-4}$ T^{-2} cm^2 mg^{-1}.

$N_D = 6400$. All amino acids are included in N_α, since the major coat proteins are close to 100% α-helical.[29,30] The molecular group diamagnetic anisotropies, $\Delta\chi_i$, are known only approximately. Worcester[31] estimates that the diamagnetic anisotropy of an α-helical peptide, $\Delta\chi_\alpha$, is 7.3×10^{-29} J T^{-2}, but Pauling[32] argues that it should be 4.45×10^{-29} J T^{-2}. As the

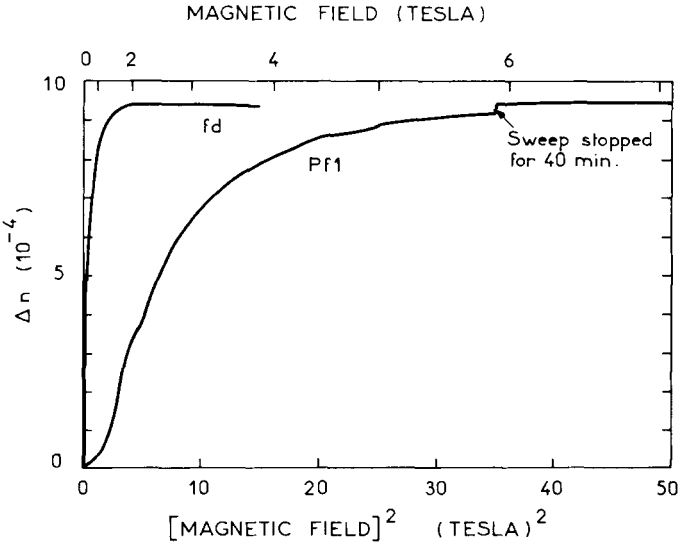

Fig. 3. Magnetic birefringence Δn of liquid-crystal-like solutions of Pf1 and fd at room temperature. The concentrations, c, are 14.8 mg/ml for Pf1 and 16.2 mg/ml for fd; the optical path length was, respectively, 0.2 and 0.1 cm. The average high-field saturation values of $\Delta n_{sat}/c$ are 6.27×10^{-5} mg^{-1} ml for Pf1 and 6.00×10^{-5} mg^{-1} ml for fd. These agree with our values obtained by wavelength variable transmission measurements (Ref. 42) on oriented samples. It is possible to make the latter measurements because, once oriented, the phage remain substantially oriented (>80%) for between 30 min and several hours, depending on concentration, vibrations, and the presence of temperature gradients. Because of the low field sweep rate used (0.037 T min^{-1}), the above curves represent the magnetic orientation at close to thermal equilibrium.

latter value is nearer the published experimental estimates,[33,34] it is used in the following analysis. This value leads to results which are consistent with other measurements on the phages, whereas the larger value does not. The $\Delta\chi$ values for tyrosine and phenylalanine have been calculated[35] to be the same as for benzene, namely, -9.6×10^{-28} J T^{-2},[25] while that of tryptophan is 1.6 times larger. Therefore, as Pf1 contains only tyrosine aromatic groups, $\Delta\chi_a$ is equal to that of benzene. In fd there is one tryptophan for every five benzene-like residues; thus, $\Delta\chi_a = -10.5 \times 10^{-28}$ J T^{-2}. By using the calculated diamagnetic anisotropy[35] for DNA bases and taking the base composition[3] into account for Pf1, $\Delta\chi_D = -4.8 \times 10^{-28}$ J T^{-2}; and for fd, $\Delta\chi_D = -4.6 \times 10^{-28}$ J T^{-2}. The $N_i\Delta\chi_i$ values can now be calculated easily, and by substituting into Eq. (6) a relationship is obtained between the three orientational factors f_i.

Bacteriophage Pf1

At room temperature Eq. (6) becomes (taking out the common factor)

$$1.22 = 1.56f_\alpha - 1.46f_a - 0.35f_D \tag{8}$$

where the measured value of $\Delta\chi$ and the calculated $N_i\Delta\chi_i$ values are used. There are many possible values of the three orientation factors which could satisfy this equation. In Fig. 4(a), f_α and f_a can have combinations of values on straight lines between and parallel to those given by the maximum and minimum values of f_D. There is no restriction on f_D, but the range of values for f_α and f_a is such that $\theta_\alpha < 47°$ and $\theta_a > 41°$. Therefore, the α-helices and the planes of the aromatic amino acid residues are, on average, likely to be more parallel than perpendicular to the virus long axis. The possible combinations of f_α and f_a are reduced to those on a single line by making use of linear dichroism data (Maret, manuscript in preparation) obtained from magnetically oriented solutions which indicate that the planes of the DNA bases are tilted so that f_D is small and negative ($\theta_D \gtrsim 60°$). With this additional restriction [$f_D = 0$ in Fig. 4(a)], θ_α ranges from 0° to 43°, while θ_a is limited to between 46° and 90°.

In the x-ray structure[12,13,16] obtained from relatively dry fibers, the average tilt of the α-helices is 18° to 20° to the virus axis. But as this angle might be larger in solution, where packing constraints are negligible and solvation could have an effect, the following estimate of the maximum tilt angle was made. In solution, the outer radius has been measured to be less than 32 Å,[36] the coat protein contains 46 residues,[8] and the residue–residue distance along an α-helix is 1.5 Å. Using this information a simple geometric calculation based on the model which has the α-helical rods of the coat protein sloping along the virus axis[12,13] gives the maximum value of $\theta_\alpha < 30°$. Thus, in solution θ_α probably lies between about 20° and 30°; then from Fig. 3 ($f_D = 0$), θ_a is between 53° and 63°.

If Pf1 is not a rigid rod as assumed but flexible,.then the $\Delta\chi$ value used in Eq. (8) is too small, and consequently the lines in Fig. 3 should be moved

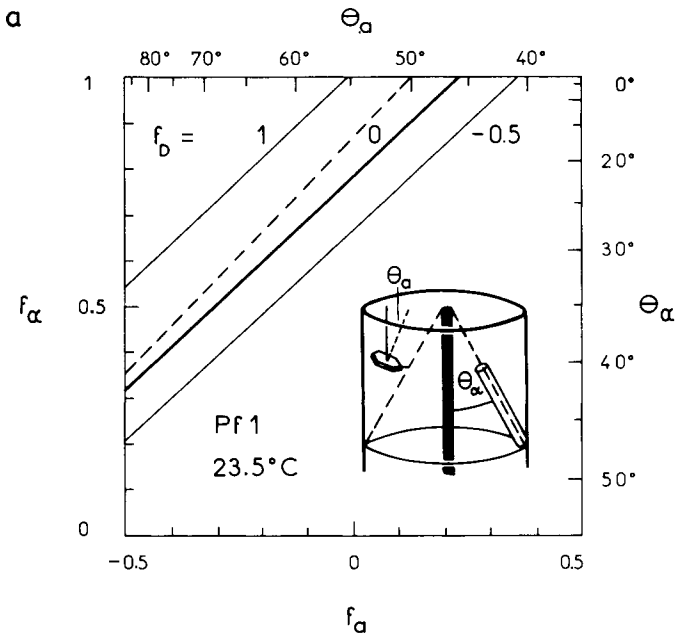

Fig. 4. Possible average orientations with respect to the virus long axis of the α-helices and aromatic amino acid residues of the major coat protein in Pf1 at 23.5°C (a) and 6.7°C (b). Inset: angles θ_α and θ_a are defined with respect to the virus long axis. f_α, f_a, and f_D are defined in the text. Lines are drawn for the largest and smallest possible values of f_D (1 and −0.5) and for the value estimated from linear dichroism, $f_D = 0$. The dashed line in (a) applies if the coat protein is only 90% α-helical.

further into the upper left-hand corner. The arguments used to restrict θ_α to 20°–30° remain valid, so if there is some flexibility, the θ_a values are larger than those estimated above. Also, if the α-helical content of the major coat protein is less than 100%, the possible orientations are reduced (Fig. 4).

The value of f_D is small, and the analysis assuming a stiff rodlike particle indicates that f_a is also small. Thus, the diamagnetic anisotropy [see Eq. (8)] comes principally from the α-helical peptide bonds. If the phages are flexible, f_a is negative, and the aromatic residues may contribute to the diamagnetic anisotropy; nonetheless the peptide-bond contribution remains dominant.

The variation of the Cotton-Mouton constant with temperature (Fig. 5) indicates that Pf1 undergoes a structural transition over a span of about 20°C. (The transition becomes sharper and less pronounced as the sample ages.) At 5°C the value is about twice that at 20°C, which means that the product $\Delta\chi\Delta\alpha$ [Eq. (4)] has doubled. If the proportional increase in both anisotropies is the same, then at 5°C their value is 1.4 times that at 20°C and Eq. (8) remains valid except that the left-hand factor is changed to 1.7 from 1.2. Figure 4(b) shows the range of possible f_a and f_α values ($\theta_\alpha < 34°$ and $\theta_a > 54°$). Again linear dichroism measurements (Maret, manuscript

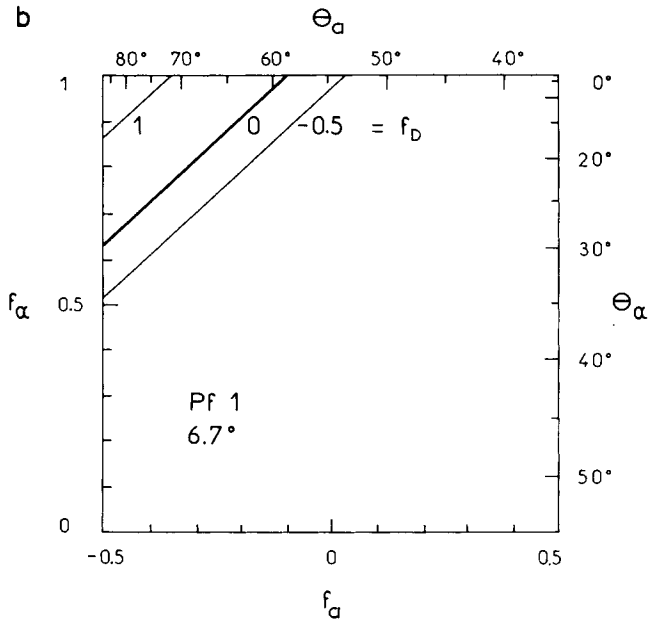

Fig. 4. (*continued from the previous page*)

in preparation) indicate that $f_D \sim 0$ at 5°C, in which case θ_α ranges from 0° to 29° and θ_a from 61° to 90°. Thus as the temperature is lowered the molecular subunits become, on average, more nearly parallel to the phage axis. It is possible that the α-helices and/or the aromatic residues have changed in orientation.

A temperature-induced transition has been observed by other means: low-angle neutron-scattering measurements of solutions[36] show that there is a 5.5% change in the mass per unit length; x-ray fiber diffraction indicates that the coat protein subunits undergo a minor rearrangement.[16] These small changes contrast with the large variation in the Cotton-Mouton constant (Fig. 5), which suggests that the method is of potential use in the study of even small structural changes. However, as this technique is also sensitive to flexibility, the temperature-induced change (Fig. 5) could be partly due to an increase in phage rigidity as the temperature is lowered. It is not possible with the data we have to differentiate between structural and/or flexibility changes.

The magnetic birefringence shows a small hysteresis (Fig. 1) at temperatures below 20°C. It could be that the magnetic field drives the structure a little in the direction of the low-temperature conformation. Perhaps a small change can be induced because there is a very small energy barrier[14] between the different conformational states and so the magnetic energy becomes significant.

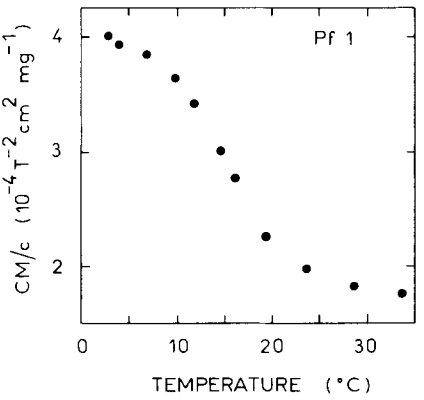

Fig. 5. Temperature dependence of the specific Cotton-Mouton constant, CM/c, of Pf1 (c = 0.08 mg/ml).

Bacteriophage fd

For fd Eq. (6) becomes

$$0.63 = 0.60f_\alpha - 1.7f_a - 0.29f_D \tag{9}$$

Figure 6 shows the span of possible values for f_α and f_a, θ_α and θ_a. The angle θ_α can take all values from 90° to 0°, while θ_a is larger than 50°. This

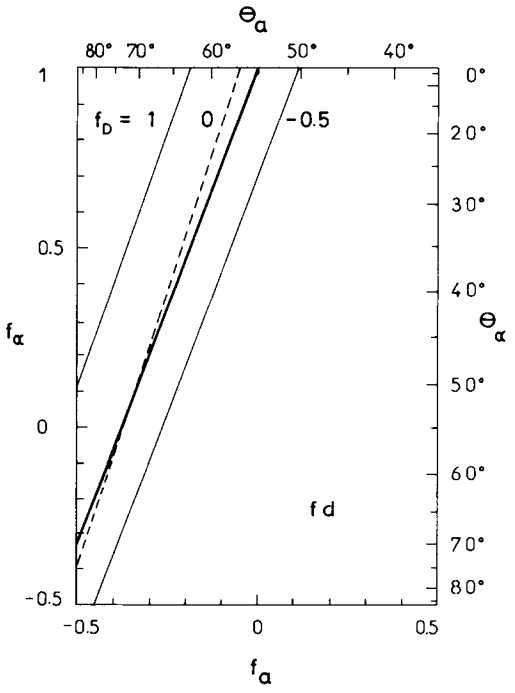

Fig. 6. As Fig. 4, but for phage fd.

means that there is no restriction on the orientation of the α-helices, but as was found for Pf1 the aromatic amino acid residues are, on average, relatively parallel to the phage axis. Linear dichroism measurements on magnetically oriented solutions of fd (Maret, manuscript in preparation) show that f_D is small and positive ($\theta_D \lesssim 50°$). Previously,[37] θ_D was estimated to be $25° \pm 5°$; however, the degree of orientation of the phages was not known accurately, and it appears to have been underestimated (Maret, manuscript in preparation). Assuming that the coat protein in fd is largely composed of axially sloping α-helical rods as in the x-ray model for Pf1,[12,13] then an upper limit to θ_α in solution is again about 30°. The additional information necessary to make this estimate is that the outer radius of the virus in solution is less than 33 Å[34] and that there are 50 amino acid residues[7] in each major coat protein. Thus, if θ_α lies (Fig. 6, $f_D = 0$) between 0° and 30°, θ_a is between 53° and 60°. Thus, as both f_a and f_D are small, the diamagnetic anisotropy of fd is due chiefly, as for Pf1, to the α-helices. If the major coat protein is less than 100% α-helical, then the factor in front of f_α in Eq. (9) is proportionally reduced. The dotted line in Fig. 6 shows that θ_a is not very sensitive to small changes in α-helical content.

Estimate of the Optical Polarizability of an α-Helical Peptide Bond

As reported above, fully aligned solutions of these phages have been produced. From the measured value of Δn_{sat}, $\Delta\alpha$, using Eq. (1), $n_0 = 1.33$ is 52.2×10^4 Å^3 for Pf1 and 21.9×10^4 Å^3 for fd. Now Eq. (7) can be used to obtain an approximate value for $\Delta\alpha_\alpha$. Both f_D and f_a are small (see above) and are put equal to zero. (For completeness we note that the optical polarizability of a DNA base and of an aromatic amino acid are probably near to that of benzene, approximately -6.0 Å^3.[24,38,39]) Firstly, assuming the shape birefringence, $\Delta\alpha_s$, is zero, we find that $\Delta\alpha_\alpha$ is, putting $\theta_\alpha = 20°$, about 1.9 Å^3 for both phages. Secondly, making use of the classical theory of Wiener[26] and taking the necessary parameters from Refs. 11 and 3, we calculate that $\Delta\alpha_s$ is about 26% of the measured $\Delta\alpha$ values; in this case, $\Delta\alpha_\alpha$ is proportionally reduced. The Wiener equation generally seems to overestimate the shape component.[26,40] As we do not have reliable values for the orientation factors and the shape contribution is unknown, we estimate that $\Delta\alpha_\alpha = 1.9 \pm 0.5$ Å^3. This is an order of magnitude larger than the value obtained from stretched keratin.[41] It is difficult to make accurate birefringence measurements of fibers; perhaps this has given rise to an underestimate.

CONCLUSIONS

It is shown that in Pf1 in solution the α-helical peptide bonds and the aromatic amino acid residues are relatively parallel to the virus long axis. Employing information from other sources, it is deduced that the α-helices

are at an angle of about 20°–30° [see insert in Fig. 4(a) for definition of angles]. This is used in conjunction with the data presented here to show that, on average, the aromatic residues lie between approximately 53° and 63° if Pf1 behaves as a rigid rod in solution and the major coat protein is 100% α-helical. Otherwise, the latter values are larger. Below room temperature, the molecular subunits are on the average more parallel to the virus axis. Both the α-helices and the aromatic residues, or only one of these groups, could have changed in average orientation with temperature. This could be combined with a decrease in flexibility. In fd the aromatic amino acid residues are also, on average, relatively parallel to the virus long axis (also reported in Ref. 37). Assuming the structure of fd is similar to the axially sloping α-helical rod model proposed for Pf1, it is concluded that the α-helices are at less than 30°, and consequently the aromatic residues lie between 53° and 60° on the average. The average angle of the aromatic groups reported above are near to, but somewhat less than, those resulting from linear dichroism measurements (Maret, manuscript in preparation).

These results demonstrate that magnetically induced birefringence can be used to investigate some general structural features in solution. The technique is particularly sensitive to changes in structure and flexibility. Unfortunately, the diamagnetic anisotropies of the molecular groups are not accurately known, and the estimate that other components do not contribute significantly may be only partly correct. In order to make the structural conclusion more reliable, measurements need to be made on model compounds to obtain sound $\Delta\chi$ values for the different groups. The main purpose of this paper is to describe in detail how the diamagnetic anisotropy of macromolecules can, in favorable circumstances, be analyzed and related to structural features. The magnetic birefringence technique has other applications, for example, it could be used to follow polymerization, reconstitution, or crystallization in strong magnetic fields.

As the orientation factors for the aromatic amino acid residues and the DNA bases, f_a and f_D, are small, the diamagnetism of both viruses comes largely from the α-helical peptide bonds. The potential importance of α-helices to magnetic orientation has been pointed out by Worcester.[31]

Finally, using the orientation factors obtained from the analysis of the diamagnetic anisotropy, we estimate that the optical anisotropy of a peptide bond is 1.9 ± 0.5 Å^3.

The experiments have been carried out at the Service National des Champs Intenses, Grenoble, and we are grateful for the support given by the personnel. We thank Dr. D. A. Marvin for the gift of virus, and M. Bichler for technical assistance. J. T. would like to thank the Deutsche Forschungsgemeinschaft for support.

References

1. Berkowitz, S. A. & Day, L. A. (1976) *J. Mol. Biol.* **102,** 531–547.
2. Newman, J. & Swinney, H. L. & Day, L. A. (1977) *J. Mol. Biol.* **116,** 593–603.
3. Wiseman, R. L., Berkowitz, S. A. & Day, L. A. (1976) *J. Mol. Biol.* **102,** 549–561.
4. Wiseman, R. L. & Day, L. A. (1977) *J. Mol. Biol.* **116,** 607–611.

5. Day, L. A. & Wiseman, R. L. (1978) *The Single-Stranded DNA Phages*, Denhardt, D. T., Dresser, D. & Ray, D. S., Eds., Cold Spring Harbor Laboratories, New York, pp. 605–625.

6. Asbeck, F., Beyreuther, K., Köhler, H., von Wettstein, G. & Braunitzer, G. (1969) *Hoppe Seyler's Z. Physiol. Chem.* **350,** 1047–1066.

7. Nakashima, Y. & Konigsberg, W. (1974) *J. Mol. Biol.* **88,** 598–600.

8. Nakashima, Y., Wiseman, R. L., Konigsberg, W. & Marvin, D. A. (1975) *Nature* **253,** 68–71 (1975).

9. Goldsmith, M. E. & Königsberg, W. H. (1977) *Biochemistry* **16,** 2686–2694.

10. Simons, G. F., Konings, R. N. H. & Schoenmakers, J. G. (1979) *FEBS. Lett.* **106,** 8–12.

11. Marvin, D. A., Wiseman, R. L. & Wachtel, E. J. (1974) *J. Mol. Biol.* **82,** 121–138.

12. Marvin, D. A. & Wachtel, E. J. (1975) *Nature* **253,** 19–23.

13. Marvin, D. A. & Wachtel, E. J. (1976) *Phil. Trans. R. Soc., Ser. B* **276,** 81–98.

14. Wachtel, E. J., Marvin, F. J. & Marvin, D. A. (1976) *J. Mol. Biol.* **107,** 379–383.

15. Makowski, L. & Caspar, D. L. D. (1978) *Single-Stranded DNA Phages*, Denhardt, D. T., Dressler, D. & Ray, D., Eds., Cold Spring Harbor Laboratories, New York, pp. 627–643.

16. Makowski, L., Caspar, D. L. D. & Marvin, D. A. (1980) *J. Mol. Biol.* **140,** 149–181.

17. Maret, G., Torbet, J., Sénéchal, E., Domard, A., Rinaudo, M. & Milas, H. (1979) *Nonlinear Behaviour of Molecules, Atoms and Ions in Electric, Magnetic or Electromagnetic Fields*, L. Néel, Ed., Elsevier, Amsterdam, pp. 477–485.

18. Torbet, J. & Maret, G. (1979) *J. Mol. Biol.* **134,** 843–845.

19. Nave, C., Fowler, A. G., Malsey, S., Marvin, D. A., Siegrist, H. & Wachtel, E. J. (1979) *Nature* **281,** 232–234.

20. Beams, J. W. (1932) *Rev. Mod. Phys.* **4,** 133–172.

21. Partington, J. R. (1953) *Advanced Treatise on Phys. Chem.*, Vol. 4, Longmans, Green, London, pp. 285–290.

22. Neurath, P. W. (1964) *Biological Effects of Magnetic Fields*, Barnothy, M. F., Ed., Plenum Press, New York, pp. 25–32.

23. Denbigh, K. G. (1940) *Trans. Faraday Soc.* **36,** 936–948.

24. Stuart, H. A. (1967) *Molekülstruktur*, Springer, Berlin.

25. Bothner-By, A. A. & Pople, J. A. (1965) *Annu. Rev. Phys. Chem.* **16,** 43–66.

26. Tsvetkov, V. N. (1964) *Newer Methods of Polymer Characterization*, B. Ke., Ed., Wiley-Interscience, New York, pp. 563–665.

27. Maret, G. & Dransfeld, K. (1977) *Physica, B, C,* **86/88,** 1077–1083.

28. Marvin, D. A. (1966) *J. Mol. Biol.* **15,** 8–17.

29. Day, L. A. (1969) *J. Mol. Biol.* **39,** 265–277.

30. Thomas, G. J. & Murphy, P. (1975) *Science* **188,** 1205–1207.

31. Worcester, D. L. (1979) *Proc. Natl. Acad. Sci. USA* **76,** 5475–5477.

32. Pauling, L. (1979) *Proc. Natl. Acad. Sci. USA* **76,** 2293–2294.

33. Tohyama, K. & Miyata, N. (1973) *J. Phys. Soc. Jpn.* **34,** 1699.

34. Murthy, N. S., Knox, J. R. & Samulski, E. T. (1976) *J. Chem. Phys.* **65,** 4835–4839.

35. Veillard, A., Pullmann, B. & Berthier, G. (1961) *C. R. Acad. Sci.* **252,** 2321–2322.

36. Torbet, J. (1979) *FEBS. Lett.* **108,** 61–65.

37. Bendet, I. J. & Mayfield, J. E. (1967) *Biophys. J.* **7,** 111–119.

38. Sokerov, S. & Weill, G. (1979) *Biophys. Chem.* **10,** 161–171.

39. Stellwagen, N. C. (1981) *Biopolymers* **20,** 399–434.

40. Tricot, M. & Houssier, C. (1976) *Polyelectrolytes*, Frisch, K. C., Klempner, D. & Patsid, A. V., Eds., Technomic Publishers, Westport, Connecticut.

41. Fraser, R. D. B. (1953) *Nature* **172,** 675–676.

42. Leenhouts, F. & van der Woude, F. (1978) *J. Phys. (Paris) Lett.* **39,** L249–L251.

Received September 2, 1980
Accepted May 15, 1981